

Measurement Data Comparison of Fast SAR Measurement System by Probe Arrays with Robot Scanning SAR Measurement System

Jun Hee Kim · Yoon-Myoung Gimm*

Abstract

Dosimetry of radiating electromagnetic wave from mobile devices to human body has been evaluated by measuring Specific Absorption Rate (SAR). Usual SAR measurement system scans the volume by robot arm to evaluate RF power absorption to human body from wireless devices. It is possible to fast estimate the volume SAR by software deleting robot moving time with the 2D surface SAR data acquired by arrayed probes. This paper shows the principle of fast SAR measurement and the measured data comparison between the fast SAR system and the robot scanning system. Data of the fast SAR is well corresponding with data of robot scanning SAR within ± 3 dB, and its dynamic range covers from 10 mW/kg to 30 W/kg with 4.8 mm probe diameter.

Key Words: 2D Array, E-Field Probe, Fast SAR, Human Safety, Radio Frequency.

I. INTRODUCTION

Evaluation of exposure of radio frequency to human body by using modern wireless devices is conducted by measuring Specific Absorption Rate (SAR).

The way to find the spatial distribution of E-field in the volume of the simulant human body is performed by robot scanning. This system takes a very long time to evaluate the SAR value of a mobile device because of robot motion to each point to access the SAR value. To promote a fast evaluation of the SAR value, 2D array of E-field probes having 3 axes isotropic characteristics was suggested [1-3].

To be a reliable fast SAR measurement system, SAR values by the fast system should give out the similar values irrespective of the measurement position of the mobile devices. Also it should yield the plausible SAR values of the

robot scanning SAR measurement system.

If the two above conditions are satisfied, a good fast SAR system should have a reasonable linearity characteristics or wide dynamic range. To confirm those performances, SAR values by RF driving position were checked and SAR values by the fast system and by robot scanning system were compared, and SAR value variations to the driving RF input power were examined.

II. CONCEPT OF SAR

SAR at a point in the lossy homogeneous medium exposed by high frequency electromagnetic field is defined in Eq. (1).

$$\text{SAR}(x, y, z) = C \left. \frac{dT}{dt} \right|_{t=0} = \frac{\sigma |\vec{E}(x, y, z)|^2}{\rho} \text{ (W/kg)}, \quad (1)$$

Manuscript received November 17 2014 ; Revised December 11 2014 ; Accepted December 22, 2014. (ID No. 20141117-062J)

Department of Electronics and Electrical Engineering, Dankook University, Yongin, Korea.

*Corresponding Author: Yoon-Myoung Gimm (e-mail: gimm@dku.edu)

This is an Open-Access article distributed under the terms of the Creative Commons Attribution Non-Commercial License (<http://creativecommons.org/licenses/by-nc/3.0>) which permits unrestricted non-commercial use, distribution, and reproduction in any medium, provided the original work is properly cited.

© Copyright The Korean Institute of Electromagnetic Engineering and Science. All Rights Reserved.

where C is specific heat capacity of the medium ($\text{J/kg} \cdot ^\circ\text{C}$), σ is electrical conductivity of the stimulant medium (S/m), $|\bar{E}|$ is electric field intensity in RMS (V/m), and ρ is mass density of the medium where SAR is to be measured (kg/m^3). Mass density in the medium $\rho(x, y, z)$ is generally set to be $1,000 \text{ kg/m}^3$ of the pure water regardless of the position or the material of the phantom for the estimation of SAR values.

Usually the SAR of the Wireless Device (WD) is estimated by volume average of Eq. (2).

$$\text{SAR}_{\text{vol avg}} = \frac{\int_V \text{SAR}(x, y, z) dV}{V} \quad (\text{W/kg}) \quad (2)$$

V in Eq. (2) is the integration volume for averaging the point SAR values in the stimulant tissue, which is usually 1 cm^3 or 10 cm^3 for 1 g or 10 g estimation in many national or international standards [4–7].

Typically the electric field to calculate SAR value is obtained by E-field probe [6]. The E-field probes consist of a set of three mutually orthogonal center-fed short dipole antennas. The E-field vector magnitude is the Root Sum Square (RSS) of the three orthogonal components by the sensors, as shown in Eq. (3).

$$|E| = \sqrt{|E_1|^2 + |E_2|^2 + |E_3|^2} \quad (3)$$

Fig. 1 shows that each sensor of the probe consists of an electrically short dipole antenna, a diode detector at the dipole feed-point, a dielectric mechanical support, and a highly resistive, RF-transparent, differential transmission line (feed-line) to extract the signal detected by the diode while maintaining the RF-transparency of the line. And a dielectric cover (typically a cylindrical low-loss plastic sleeve) encloses the probe for chemical and mechanical protection. Fig. 2

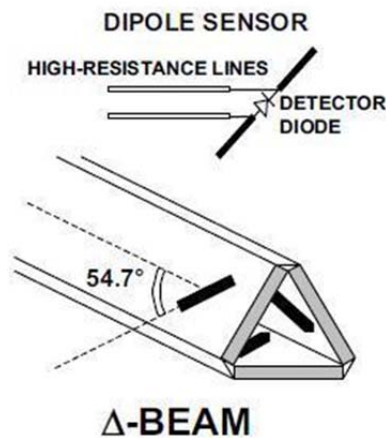


Fig. 1. Typical E-field probe construction of a ‘ Δ -beam’ (or ‘triangular-beam’) dielectric structure supports the three miniature and mutually orthogonal sensor dipoles.

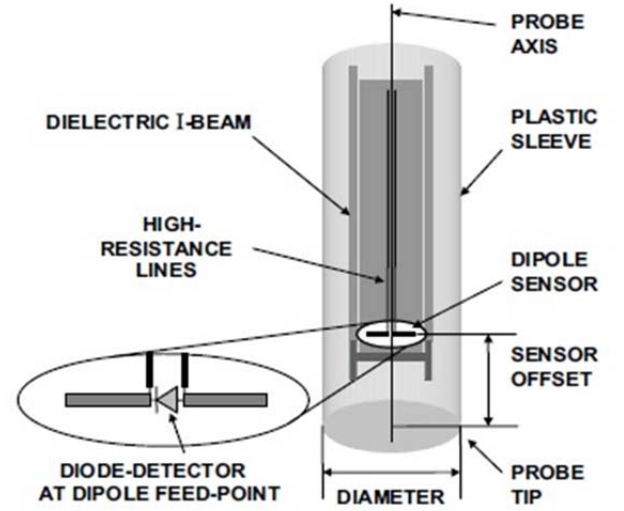


Fig. 2. E-field probe features. Sensor offset is measured from the geometric center of the sensors to the tip of the probe enclosure.

shows E-field probe relevant features [8].

The basic principles of 3D SAR estimation from 2D data are based on the exponential decay of the propagating field in the heavily loss medium. The SAR at an arbitrary point can be simply expressed by Eq. (4) if the characteristics of the incident wave behave like an attenuating planar wave [9].

$$\begin{aligned} \text{SAR}(x, y, z) &= \text{SAR}(x, y, 0)e^{-2z/\delta} \\ &= \text{SAR}(x, y, z_d)e^{-2(z-z_d)/\delta}, \end{aligned} \quad (4)$$

where δ is penetration depth of the medium at an angular frequency ω , and z_d is detecting diode position in Fig. 3. Wave penetration depth in the medium is given by,

$$\delta = \frac{1}{\omega \sqrt{(\mu_0 \epsilon_r \epsilon_0 / 2) \left(\sqrt{1 + \left(\frac{\sigma}{\omega \epsilon_r \epsilon_0} \right)^2} - 1 \right)}} \quad (5)$$

Because it is not convenient to exchange repeatedly the internal phantom material of this fast SAR measurement system by the different measurement frequency, it is favorable that the human-simulating media have properties of very wide bandwidth satisfying the artificially required dielectric permittivities and electric conductivities.

Considering the exponential decay of the radiating field in the medium, the peak volume average SAR to be estimated in a volume V is expressed by Eq. (6).

$$\begin{aligned} \text{SAR}_{\text{vol avg}} &= \frac{1}{V} \iiint_{V_{\text{max}}} \text{SAR}(x, y, z_d) e^{-2(z-z_d)/\delta} dx dy dz \end{aligned} \quad (6)$$

where z_d is again the position of the field detecting sensors in the medium. If V is a cube of L_c in Fig. 3, the SAR will be calculated by Eq. (7).

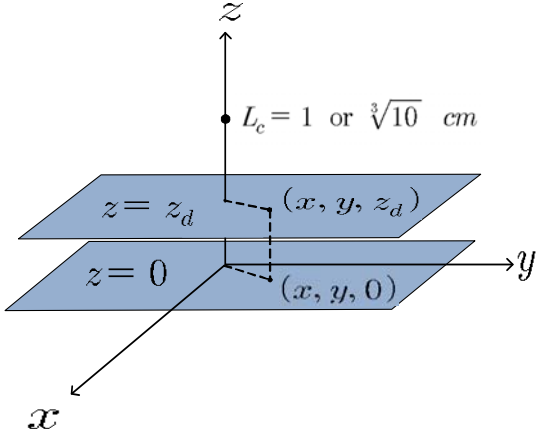


Fig. 3. Conceptual structure of a phantom shell plane ($z = 0$), and probe sensor plane ($z = z_d$). L_c is the length of the cube for 1 g or 10 g volume average, where peak volume SAR is to be estimated.

$$\begin{aligned} \text{SAR}_{\text{vol avg.}} &= \frac{1}{L_c^2} \iint_{A_{\text{max}}} \text{SAR}(x, y, z_d) dx dy \cdot \frac{1}{L_c} \int_0^{L_c} e^{-\frac{2(z-z_d)}{\delta}} dz \\ &= \frac{\delta}{2L_c^3} e^{\frac{2z_d}{\delta}} \left(1 - e^{-\frac{2L_c}{\delta}}\right) \iint_{A_{\text{max}}} \text{SAR}(x, y, z_d) dx dy \\ &= K(\omega, \epsilon_r, \sigma, L_c, z_d, \delta) \iint_{A_{\text{max}}} \text{SAR}(x, y, z_d) dx dy \quad (7) \end{aligned}$$

A_{max} in Eq. (7) is the planar or curved square surface of L_c in the medium which contains the maximum point SAR position.

All of the planar data $\text{SAR}(x, y, z_d)$ are acquired by the neighboring multiple probes of 15-mm apart with 4.8 mm diameter in this research for the sampling, and the data are interpolated by bicubic interpolation algorithm which guarantees continuity of the first gradient and cross-derivative. Probe neighboring distance (15 mm) was deliberately decided between the perturbation error by probe volume in the phantom medium and data interpolation error between the neighboring probes. It has been found that a 20 mm \times 20 mm measurement grid is usually sufficient to achieve the required interpolation accuracy for locating SAR peaks within 5 mm when two staggered one-dimensional cubic splines are used to estimate the maximum SAR location [6, 10]. Probe neighboring distance should be greater than the diameter of the probes for proper arrays. If the distance between the neighboring probes becomes larger, the interpolated datum for each point SAR would have more inaccuracy.

It is very difficult to measure the coupling level between the two neighboring probes. The length of dipole antennas in the probe is so short and the environmental liquid bet-

ween the probes are very lossy, we assume the mutual coupling between the neighboring probes are negligible. After interpolation process, re-sampled data by a 1-mm step are calculated to give a 2D planar point SAR for the volumetric calculation by Eq. (7).

III. PERFORMANCE CHECK OF FAST SAR MEASUREMENT SYSTEM

1. Structure of Fast SAR Measurement System

Fast SAR measurement system sets probes in array by constant interval in SAM phantom or in body phantom to calculate volume SAR of peak 1 g and 10 g without robot scanning. Figs. 4 and 5 show the probe array dispositions in the generally used phantom shapes. The probes referred to Section II are submerged in a solution which is a simulant human liquid with the wide bandwidth (0.4–6 GHz) characteristic [11]. And the probes are connected with the electronic circuits and a computer which calculates SAR values by the predetermined software. The Devices Under Tests (DUTs) contact with the plastic phantom surface when they are measured following to the international standards [5-7].

2. Homeostasis of SAR Values to the Measurement Positions

Because of the sparse data in the phantom space by the arrayed probes in fast SAR system, it is important to check SAR value variation following to the DUT positions.



Fig. 4. Probe array disposition in the right SAM phantom.

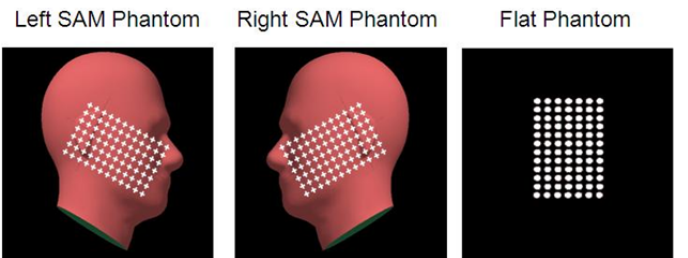


Fig. 5. Positions of E-field sensors in tissue-simulating medium in the left SAM, right SAM, and flat phantoms.

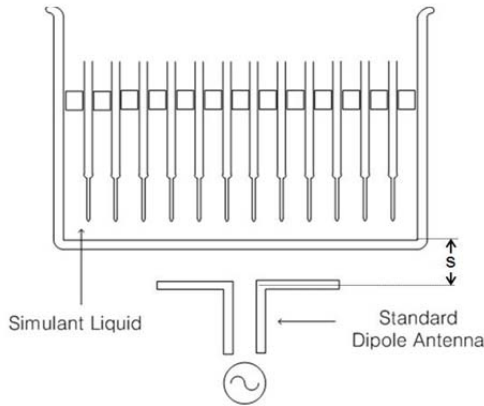


Fig. 6. Performance check of fast SAR measurement system.

Table 1. Data of the fast specific absorption rate (SAR) measurement system at 1,900 MHz

Test condition	
Frequency	1,900 MHz
Dielectric constant	40.0
Conductivity	1.40 S/m
Phantom model	Flat
Input RF power	24 dBm (0.25 W)
Distance of the dipole to the phantom (s)	10 mm
Measured and calculated data	
Measured peak 1 g SAR	9.89–9.94 W/kg
Numerical peak 1 g SAR	9.93 W/kg
Measured peak 10 g SAR	5.12–5.16 W/kg
Numerical peak 10 g SAR	5.13 W/kg

Test result of SAR values depending on measurement points with 250 mW (24 dBm) RF signal fed by a standard dipole antenna shown in Fig. 6 is summarized in Table 1. All of the test arrangements, geometrical distances and a radiator or phantom structures follow the international standards for system validation [6, 7]. Although 1.9 GHz is chosen as the test frequency in this paper, the usability of the fast SAR measurement can be extended to lower 300 MHz and to upper 3 GHz which will include most of the modern mobile devices, with wider band probes and wider band simulant liquid. The field intensity contour pattern and SAR values are satisfactorily maintained regardless of the radiating dipole antenna positions in Fig. 7 to the arbitrary same input powers.

SAR values are measured to be in the range of 9.89–9.94 W/kg and 5.12–5.16 W/kg in terms of peak 1 g and 10 g average, respectively. The dominant factor of these measurement variation is due to the position change of the radiating dipole antenna.

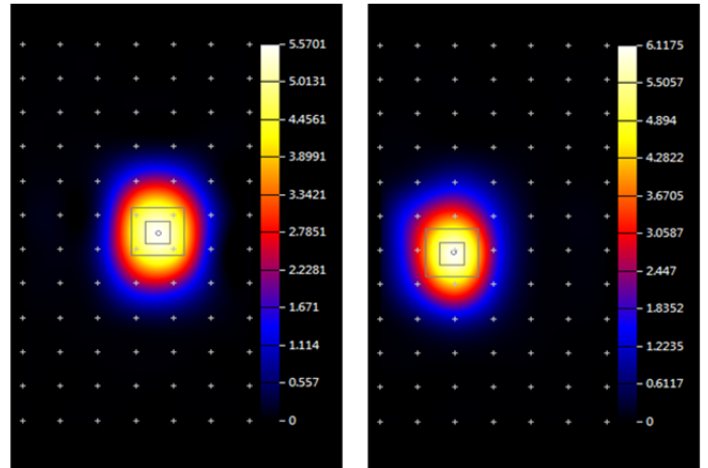


Fig. 7. SAR field intensity contour patterns of a fast SAR measurement system in the flat phantom at 1,900 MHz with the different dipole antenna positions. Left and right figures are the patterns when the center positions of the radiating dipoles are at different positions each other under the flat phantom. Numbers of the color bars are point SAR values in W/kg.

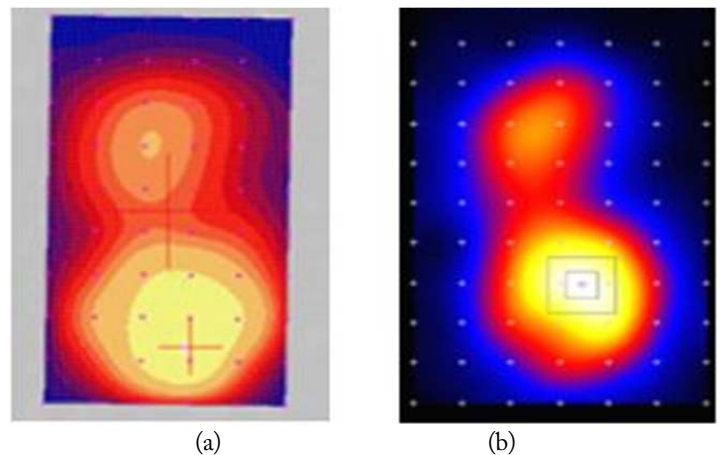


Fig. 8. SAR distribution contours of a WCDMA mobile phone. (a) SAR contour by robot SAR, (b) SAR contour by fast SAR system.

3. Measurement Data Comparison of SAR Values between Robot Scanning SAR and Fast SAR Systems

Fig. 8 shows SAR distribution contour comparison between the robot scanning system and fast SAR system of a WCDMA mobile phone. Both distributions coincide pretty well not only in major peak area but also in less intense area. Measured data by robot scanning system is 0.666 (1 gram) and 0.356 (10 gram) W/kg each, while they are 0.6085 (1 gram) and 0.3811 (10 gram) W/kg each by fast SAR system.

Fig. 9 shows SAR values comparison by the robot scanning system and by the fast SAR system of WCDMA mobile phones. Each SAR value is under blue line and above gray line which means that the difference of robot scanning SAR value and fast SAR value are within +3 and -3 dB.

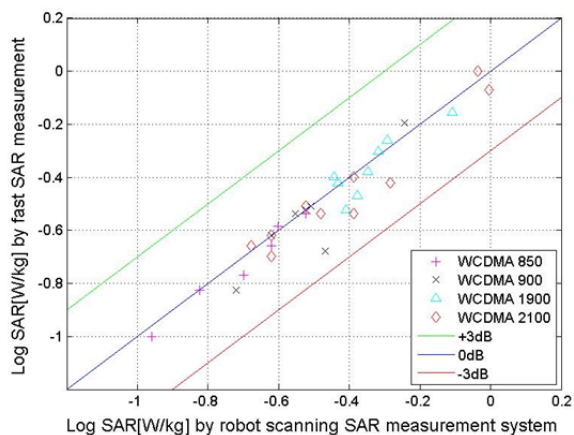


Fig. 9. Comparison between logarithmic fast SAR values and robot scanning SAR values of WCDMA phones with the left SAM phantom.

4. Linearity Characteristics of fast SAR Measurement System

RF power from 0 dBm (1 mW) to 39 dBm (8 W) by 3 dB step was driven to a dipole antenna for linearity response test of the fast SAR measurement system at 1,900 MHz. Fig. 10 shows lines of measured data of 1 g and 10 g SAR by fast SAR system, and it shows that 1 g and 10 g SAR lines are parallel and straight in 9–27 dBm input range. Nonlinear characteristics are observed out of this linear range. The reasons of nonlinear region by the low or high input power conditions are due to the detection limit of the sensor or of the system.

Improved linear characteristics at high input power region can be obtained by using thinner diameter probes than 4.8 mm such as 3.0 mm diameter.

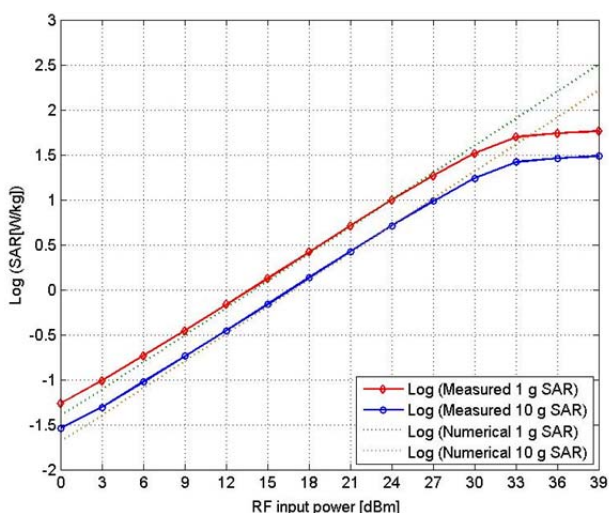


Fig. 10. Logarithmic fast SAR values to the increasing RF input power from 0 dBm to 39 dBm at 1,900 MHz to check the linearity of the fast SAR system.

IV. CONCLUSION

Some important performances of fast SAR measurement system with stationary multiple E-field sensor arrays (7×12) were checked at 1,900 MHz. This system produced similar SAR values irrespective of horizontal measurement position of mobile device. Measured SAR values well coincide with the robot scanning SAR value within ± 3 dB. And it has a good linearity characteristics if input power is under 1 W. If better linearity is required at higher SAR (>10 W/kg) realm, a thinner diameter probe with lower sensitivity can be used.

Judging from the results of this study, fast SAR measurement system can be substitutive for the robot scanning system to measure SAR values of WCDMA mobile devices. It needs more tests at other frequencies for reliability evaluation of this fast SAR measurement system with different probe diameters. This fast SAR system is efficiently used for SAR measurements of LTE phones which have about a hundred test modes for a single mobile device. The main purpose of using this fast SAR system for LTE phones is to find out the parameter conditions which give the maximum SAR of the phones.

This work was supported by the ICT R&D program of MISP/IITP, Republic of Korea (13-911-01-106, Development of Human Exposure Measurement System to EMF from Wireless Devices Close to Human Body).

REFERENCES

- [1] Y. M. Gimm, and D. H. Kwon, "Fast SAR measurement system structure using E-field sensors array," in *Proceedings of 2010 Asia-Pacific Radio Science Conference (AP-RASC)*, Toyama, Japan, 2010.
- [2] Y. M. Gimm, Y. Ju, S. Kahng, Y. Lee, and S. Lee, "Quick SAR measurement system by 2D array E-field sensors," in *Proceedings of Asia-Pacific Microwave Conference (AP-MC)*, Seoul, Korea, 2013, pp. 383–385.
- [3] Y. M. Gimm, and S. B. Lee, "Analysis of the SAR value by probe array," in *Proceedings of 2014 KIEES Summer General Conference*, Jeju, Korea, 2014, p. 90.
- [4] International Commission on Non-Ionizing Radiation Protection, "ICNIRP statement on the 'guidelines for limiting exposure to time-varying electric, magnetic, and electromagnetic fields (up to 300 GHz)," *Health Physics*, vol. 97, no. 3, pp. 257–258, 2009.
- [5] R. F. Cleveland, D. M. Sylvar, and J. L. Ulcek, "Evaluating compliance with FCC guidelines for human exposure to

- radiofrequency electromagnetic fields," *OET Bulletin 65 (Edition 97-01)*, Standards Development Branch, Allocations and Standards Division, Office of Engineering and Technology, Federal Communications Commission, Washington, DC, 1997.
- [6] IEEE Recommended Practice for Determining the Peak Spatial-Averaged Specific Absorption Rate (SAR) in the Human Head from Wireless Communication Devices: Measurement Techniques, IEEE Standard 1528-2003.
- [7] Human exposure to radio frequency fields from handheld and body-mounted wireless communication devices - Human models, instrumentation, and procedures - Part 2: Procedure to determine the specific absorption rate (SAR) for mobile wireless communication devices used in close proximity to the human body (frequency range of 30 MHz to 6 GHz), IEC 62209-2/FDIS, 2009.
- [8] A. Faraone, D. O. McCoy, C. K. Chou, and Q. Balzano, "Characterization of miniaturized E-field probes for SAR measurements," in *Proceedings of IEEE International Symposium on Electromagnetic Compatibility*, Washington, DC, 2000, pp. 749-754.
- [9] M. Y. Kanda, M. G. Douglas, E. D. Mendivil, M. Ballen, A. V. Gessner, and C. K. Chou, "Faster determination of mass-averaged SAR from 2-D area scans," *IEEE Transactions on Microwave Theory and Techniques*, vol. 52, no. 8, pp. 2013-2020, 2004.
- [10] T. Schmid, O. Egger, and N. Kuster, "Automated E-field scanning system for dosimetric assessments," *IEEE Transactions on Microwave Theory and Techniques*, vol. 44, no. 1, pp. 105-113, 1996.
- [11] B. Loader, A. Gregory, D. Bowns, and Y. Johnson, "Non-toxic phantoms for SAR measurements (30 MHz to 6 GHz)," in *Proceedings of the 32nd Annual Meeting of the Bioelectromagnetics Society (BEMS)*, Seoul, Korea, 2010, p. 94.

Jun Hee Kim



received the B.E. degree in electronics and electrical engineering from Dankook University in 2014. He is currently a M.S. candidate in electronics and electrical engineering, Graduate School, Dankook University. His research interests are the electromagnetic field measurement related with the human safety and wireless power transfer.

Yoon-Myoung Gimm



received the B.E. degree in electronics engineering from the Seoul National University, Seoul, Korea, in 1975, and the M.S and Ph.D. degrees in electrical and electronics engineering from Korea Advanced Institute of Science and Technology (KAIST) in 1977 and 1990, respectively. Since 1980, he has been in the department of electronics engineering, Dankook University, where he is now a professor in the school of electronics and electrical engineering. He is also a CEO of EMF Safety Inc. since 2000. His research interests are the electromagnetic field measurement related with the biological effect and human safety.